Polyhedron 31 (2012) 167–175

Contents lists available at SciVerse ScienceDirect

Polyhedron

journal homepage: www.elsevier.com/locate/poly

Encapsulating ruthenium and osmium with tris(2-aminoethyl)amine based tripodal ligands

Soumik Mandal [a], Dipravath K. Seth [b], Parna Gupta [a,*]

[a] Department of Chemical Sciences, Indian Institute of Science Education and Research, Kolkata, BCKV Main Post Office, Mohanpur 741252, West Bengal, India
[b] Department of Chemistry, Inorganic Chemistry Section, Jadavpur University, Kolkata 700032, India

ARTICLE INFO

Article history:
Received 21 July 2011
Accepted 7 September 2011
Available online 17 September 2011

Keywords:
Ru/Os-complex
Tris(2-aminoethyl)amine Schiff base
Coordination cage
Fluorescence
DFT calculation
Geometry optimization

ABSTRACT

The reaction of a series of tripodal ligands, $H_3L^{1,2}$ and L^{3-6}, with $[M(PPh_3)_2Cl_2]$ (M = Ru, Os) affords a family of coordination cage compounds of the type $[M^{III}L^{1,2}]$ (**1–4**) or $[M^{II}L^{3-6}](BPh_4)_2$ (**5–12**). The Schiff base ligands (H_3L^1, L^3, L^5) have been synthesized by condensation of tris(2-aminoethyl)amine with salicylaldehyde, pyridine-2-aldehyde and 1-methyl-2-imidazolecarboxaldehyde. These ligands were further reduced and subsequently methylated to form the new ligands (H_3L^2, L^4, L^6). Single crystal X-ray diffraction studies of **1** and **2** show that the tripodal ligand wraps around the metal center as a hexadentate ligand to form a cage. All the synthesized compounds have been thoroughly characterized by ESI-MS, FT-IR, UV–Vis and NMR spectroscopic methods. To the best of our knowledge, this is the first ever report of osmium complexes with tris(2-aminoethyl)amine based tripodal ligands. DFT calculations were performed to obtain geometry optimized structures of all the other complexes (**3–12**).

1. Introduction

The importance of tripodal tetraamine ligands in coordination chemistry has been amply demonstrated over many years [1–4]. A large number of such ligands, also known as podands, have been prepared, and metal complexes containing these ligands have been shown to exhibit a wide variety of physical and chemical properties [5,6]. The binding sites in these podands are hard (mostly N and O), and therefore stabilize transition metal centers very well [7–10]. They have drawn much attention in recent years, mainly due to their possession of spheroidal cavities which enable them to efficiently sequester metal ions. They also have demonstrated their potential use in the synthesis of polynuclear structures [11–16].

Tris(2-aminoethyl)amine is one of the most rigorously used tripodal tetramine frameworks, due to its variable coordination modes leading to variety of structural assembles [17–21]. It was first synthesized long ago, dating back to 1896 [22], and it is still highly relevant, due to its versatility as a ligand, and also for the interesting applications of its complexes in the synthesis of novel materials [23–25] and medicine [26–28]. One of the ways in which the basic ligand skeleton of a tripodal tetraamine ligand can be altered is the formation of Schiff bases [29–33]. The metal complexes of Schiff bases based on tris(2-aminoethyl)amine are very interesting as they show good anion receptive properties [34] and emission patterns [35–37]. The interesting photophysical properties help these classes of complexes to find application in molecular recognition [38,39].

The tris(2-aminoethyl)amine molecule has a flexible tripodal structure with three aminoethyl groups showing multidentate coordination modes. Interestingly, the coordination chemistry of the tris(2-aminoethyl)amine Schiff base based tripodal ligand has remained largely unexplored. A literature survey shows that the chemistry of this type of ligand with the 4d series of metals, except ruthenium, is not so well known [40,41]. In the present study, tris(2-aminoethyl)amine is allowed to react with salicylaldehyde, pyridine-2-aldehyde and 1-methyl-2-imidazolecarboxaldehyde to form Schiff bases, then these ligands were further reduced and subsequently the imine(–CH=N–) nitrogen atoms were methylated. All six ligands (Fig. 1) were allowed to react with ruthenium and osmium precursors to form coordination cage [42,43] complexes through N,O or N,N chelating atoms. This study reports the first synthesis and complete characterization of osmium complexes with tris(2-aminoethyl)amine based ligands. All the complexes are expected to be chiral because of the spiral coordination arrangement of the achiral ligands around the metal. The CD spectra of $[RuL^1]$ (**1**), $[OsL^1]$ (**2**) and $[RuL^2]$ (**3**) indicate the presence of a racemic mixture for each in solution, as expected. Interestingly, there are considerable changes in the emission pattern as well as the wavelength of emission between these ligands and their corresponding complexes. DFT calculations were performed to obtain geometry optimized structures of the ruthenium ($[RuL^2]$ (**3**), $[RuL^3(BPh_4)_2]$ (**5**), $[RuL^4(BPh_4)_2]$ (**7**), $[RuL^5(BPh_4)_2]$ (**9**)

* Corresponding author. Tel.: +91 3473279130; fax: +91 3473279131.
E-mail address: parna.gupta@gmail.com (P. Gupta).

0277-5387/$ - see front matter © 2011 Elsevier Ltd. All rights reserved.
doi:10.1016/j.poly.2011.09.010

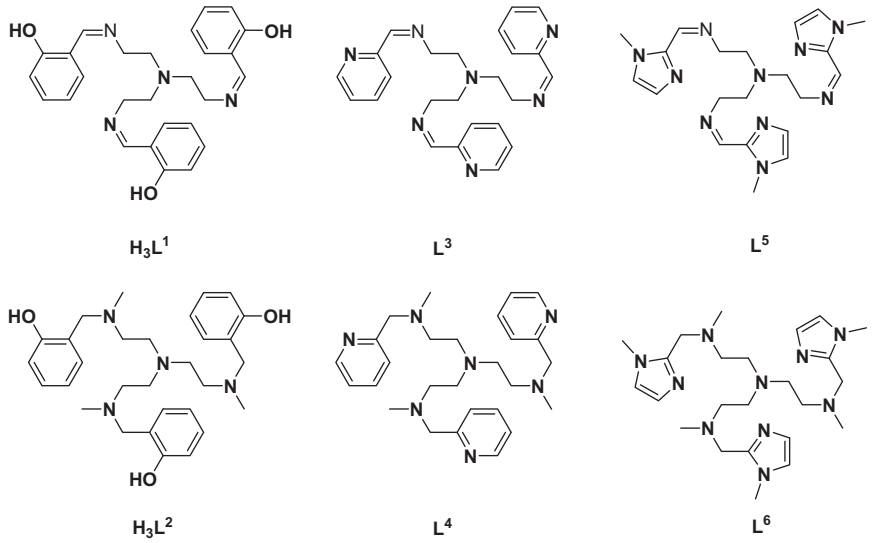

Fig. 1. Schematic diagram of the ligands $H_3L^{1,2}$, L^3–L^6.

and $[RuL^6(BPh_4)_2]$ (**11**)) and osmium ($[OsL^2]$ (**4**), $[OsL^3(BPh_4)_2]$ (**6**), $[OsL^4(BPh_4)_2]$ (**8**), $[OsL^5(BPh_4)_2]$ (**10**) and $[OsL^6(BPh_4)_2]$ (**12**)) complexes and to establish the nature of the orbitals involved in the transition processes and to correlate the structural parameters with the spectroscopic properties of the complexes. An account of the chemistry of the complexes of the tris(2-aminoethyl)amine based tripodal ligands is presented here, with special reference to their formation, structure and spectral and electrochemical properties.

2. Experimental

2.1. Materials and methods

The starting materials $RuCl_3.3H_2O$, $(NH_4)_2[OsCl_6]$, tris(2-aminoethyl)amine, salicylaldehyde, pyiridine-2-aldehyde, 1-methyl-2-imidazolecarboxaldehyde and triphenylphosphine were purchased from Sigma–Aldrich and were used without purification. All the solvents were dried by the usual methods prior to use. $[Ru(PPh_3)_3Cl_2]$, $[Ru(CO)_2(PPh_3)_2Cl_2]$ and $[Os(PPh_3)_3Cl_2]$ were prepared according to the reported procedures [44–46].

2.2. Synthesis of the ligands

2.2.1. H_3L^1

To a solution of salicylaldehyde (1 g, 8.20 mmol) in ethanol (20 mL) was added tris(2-aminoethyl)amine (0.40 g, 2.73 mmol) in absolute ethanol (20 mL). A yellow precipitate was formed immediately. The mixture was refluxed and stirred for 2 h, the resulting solid was filtered off, washed with diethyl ether, and dried in air to obtain the desired compound.

Yield 1.13 g (90%); *Anal.* Calc. for $C_{27}H_{40}N_4O_3$: C, 69.20; H, 8.60; N, 11.96. Found: C, 69.10; H, 8.80; N, 11.90%; ESI-MS *m/z*: 458.88 (M^+), 311.87 $(M–CH_2CH_2N{=}CHPhOH)^+$, 165.99 $(M^+–\{CH_2CH_2N{=}CHPhOH\}_2)^+$; ^1H NMR (400 MHz, $CDCl_3$, δ, ppm): 2.75 (m, 6H), 3.45 (m, 6H), 5.98 (d, 3H), 6.50 (t, 3H), 6.84 (t, 3H), 7.18 (t, 3H), 7.72 (s, 3H); ^{13}C NMR (500 MHz, $CDCl_3$, δ, ppm): 166.09 (N=C), 116.68 (aromatic ring), 118.48 (aromatic ring), 131.75 (aromatic ring), 161.05 (aromatic ring), 57.89 (NCH_2CH_2), 55.80 (NCH_2CH_2); IR (cm^{-1}, KBr pellet): 3436 (b, νO–H, typical for intramolecular hydrogen bonded O–H), 3000–2800 (ν_{C-H}), 1632 ($\nu_{C=N}$), 1610, 1582, 1498, 1459, 1430, 1337, 756.

2.2.2. L^3

To a solution of pyridine-2-aldehyde (1 g, 9.34 mmol) in ethanol (20 mL) was added tris(2-aminoethyl)amine (0.46 g, 3.11 mmol) in dry toluene (50 mL). The mixture was refluxed and stirred overnight, and the resulting liquid evaporated to dryness, affording an oily substance. The oily mass upon washing with cold ethanol gives the pure ligand.

Yield: 0.64 g (50%); *Anal.* Calc. for $C_{24}H_{27}N_7$: C, 69.71; H, 6.58; N, 23.71. Found: C, 69.45; H, 6.55; N, 23.92%; ESI-MS *m/z*: 414.83 $(M)^+$, 147.94 $(NCH_2CH_2N{=}CHPy)^+$. ^1H NMR (400 MHz, $CDCl_3$, δ, ppm): 10.05 (–CH, 3H), 8.57 (3H, d, aromatic ring), 7.6–8.35 (9H, aromatic ring), 3.76 (6H, t, NCH_2CH_2), 2.96 (6H, t, NCH_2CH_2); ^{13}C NMR (500 MHz, $CDCl_3$, δ, ppm): 162.64 (N=C), 154.38 (aromatic ring), 149.24 (aromatic ring), 136.44 (aromatic ring), 124.52 (aromatic ring), 121.18 (aromatic ring), 59.73 (NCH_2CH_2), 55.22 (NCH_2CH_2). IR (cm^{-1}, KBr pellet): 3435–2850 (ν-H), 2850, 1651 ($\nu_{C=N}$), 1587, 1469, 1436, 774.

2.2.3. L^5

To a solution of 1-methyl-2-imidazolecarboxaldehyde (1 g, 9.08 mmol) in dry methanol (50 mL) was added tris(2-aminoethyl)amine (0.44 g, 3.01 mmol) in dry toluene (50 mL). The mixture was refluxed and stirred for overnight, and then the resulting liquid was purified by column chromatography. Yield 0.96 g (76%); *Anal.* Calc. for $C_{21}H_{30}N_{10}$: C, 59.69; H, 7.16; N, 33.15. Found: C, 60.01; H, 7.25; N, 33.08%; ESI-MS *m/z*: 422.89 $(M)^+$; ^1H NMR (400 MHz, $CDCl_3$, δ, ppm): 2.88–2.92 (br, 6H, NCH_2CH_2), 3.64–3.67 (br, 6H, NCH_2CH_2), 3.89 (s, 9H, N-CH_3), 6.86 (d, 3H, imidazole ring), 7.04 (d, 3H, imidazole ring), 8.25 (s, 3H, CH); ^{13}C NMR (500 MHz, $CDCl_3$, δ, ppm): 153.77 (N=C), 142.96 (imidazole ring), 128.92 (imidazole ring), 124.63 (imidazole ring), 60.25 (NCH_2CH_2), 55.29 (NCH_2CH_2), 35.15 (N–CH_3); IR (cm^{-1}, KBr pellet): 3400–2352 (ν-H), 1651 ($\nu_{C=N}$), 1479, 1439, 1288, 764.

2.2.4. Synthesis for H_3L^2, L^4 and L^6

H_3L^2, L^4 and L^6 were prepared by similar procedures [47]. A detailed method is given for one representative case.

To a solution of H_3L^1 (0.50 g, 1.09 mmol) in dry methanol, $NaBH_4$ (0.22 g, 6 mmol) was added slowly at low-temperature (~5 °C). The mixture was stirred overnight at room temperature. The solvent was evaporated and 20 mL water was added. The aqueous solution was treated with dilute hydrochloric acid until pH 7–8 was reached. The solution was extracted with dichloromethane

and dried over anhydrous Na_2SO_4. The reduced amine was obtained as a colorless solid (orange and pale yellow liquids from L^3 and L^5, respectively). To a solution of the amine in dichloromethane, formaldehyde (0.18 g, 6 mmol) was added with stirring. Sodium acetoxyborohydride (2.12 g, 10 mmol) was added to this mixture, which was subsequently stirred for 24 h. The solution was neutralized with K_2CO_3 solution. The organic layer was washed with water and separated with a separating funnel and dried over fused Na_2SO_4. Removal of the solvent afforded pure H_3L^2 (or L^4 and L^6 from L^3 and L^5, respectively).

2.2.5. H_3L^2

Yield: 0.342 g, 61%; *Anal.* Calc. for $C_{29}H_{40}N_4O_3$: C, 70.70; H, 8.18; N, 11.37. Found: C, 70.85; H, 8.12; N, 11.27%; ESI-MS *m/z*: 506.77 (M^+), 400.87 $[M-(CH_2PhOH)]^+$; ^{1}H NMR (400 MHz, $CDCl_3$, δ, ppm): 2.22 (s, 9N–CH_3), 2.52–2.63 (complex, 12H), 3.66 (s, 6CH_2), 6.74–7.18 (12H, aromatic); ^{13}C NMR (500 MHz, $CDCl_3$, δ, ppm): 157.75 (salicylaldehyde C–OH), 128.73 (aromatic ring), 128.52 (aromatic ring), 121.92 (aromatic ring), 119.0 (aromatic ring), 116.01 (aromatic ring), 61.12 (N–CH_2–aromatic ring), 54.30 (N–CH_2CH_2), 52.13 (N–CH_2CH_2), 41.87 (N–CH_3); IR (cm^{-1}, KBr pellet): 3436 (b, νO–H, typical for intramolecular hydrogen bonded O–H), 3000–2817 (ν_{C-H}), 1589, 1488, 1256 (νN–C), 754.

2.2.6. L^4

Yield: 0.317 g, 57%; *Anal.* Calc. for $C_{27}H_{39}N_7$: C, 70.25; H, 8.52; N, 21.24. Found: C, 70.21; H, 8.46; N, 21.22%; ESI-MS *m/z*: 461.97 (M^+); ^{1}H NMR (400 MHz, $CDCl_3$, δ, ppm): 2.16 (s, 9N–CH_3), 2.47 (complex, 6H), 2.59 (complex, 6H), 3.58 (s, 6CH_2), 8.46 (d, 3H), 7.56 (t, 3H), 7.33 (d, 3H), 7.08 (t, 3H); ^{13}C NMR (500 MHz, $CDCl_3$, δ, ppm): 159.01 (aromatic ring adjacent to pyridine N), 148.86 (aromatic ring adjacent to pyridine N), 136.31 (aromatic ring), 123.03 (aromatic ring), 121.86 (aromatic ring), 64.02 (N–CH_2–aromatic ring), 55.29 (N–CH_2CH_2), 52.60 (N–CH_2CH_2), 42.76 (N–CH_3); IR (cm^{-1}, KBr pellet): 3389–2352 (νN–H), 1591, 1471, 1434, 1361, 1297 (νN–C), 1034, 760.

2.2.7. L^6

Yield: 0.294 g, 52%; *Anal.* Calc. for $C_{24}H_{42}N_{10}$: C, 61.25; H, 8.99; N, 29.76. Found: C, 61.23; H, 9.05; N, 29.89%; ESI-MS *m/z*: 470.96 (M^+), 456.97 $[M^+–CH_3]^+$, 331.89 $[M^+–(CH_2N(Me)CH_{2(imidazole)})]^+$; ^{1}H NMR (400 MHz, $CDCl_3$, δ, ppm): 6.75–6.87 (imidazole ring, complex), 4.66 (s, 3CH_2), 3.63 (s, 9CH_3), 2.39–2.46 (12H, NCH_2CH_2), 2.14 (s, 9CH_3); ^{13}C NMR (500 MHz, $CDCl_3$, δ, ppm): 145.13 (imidazole ring), 126.67 (imidazole ring), 121.45 (imidazole ring), 54.54 (N–CH_2–aromatic ring), 54.14 (NCH_2CH_2), 52.04 (NCH_2CH_2), 42.06 (N–CH_3), 32.86 (N–CH_3, aromatic ring); IR (cm^{-1}, KBr pellet): 3401–2360 (ν_{N-H}), 1568, 1501, 1455, 1284, 1025, 801, 755.

2.3. Synthesis of the complexes

*2.3.1. $[RuL^1]$ (**1**)*

To a hot solution of H_3L^1 (0.046 mg, 0.10 mmol) and triethylamine (0.30 g, 0.3 mmol) in warm ethanol (40 mL) was added $[Ru(PPh_3)_2Cl_2]$ (0.096 g, 0.10 mmol). The mixture was heated at reflux for 24 h to produce a dark brownish-orange solution. Stripping of the solvent from the solution under vacuum gave a brownish-orange solid, which was subjected to thin-layer chromatography on a silica plate. With acetonitrile:toluene (1:4) as the eluant, a green band separated out. The green band was extracted with acetonitrile, and slow evaporation of the acetonitrile extract gave a green crystalline solid of the composition $[RuL^1]$. Yield: 0.073 g, 60%. *Anal.* Calc. for $C_{27}H_{27}N_4O_3Ru$: C, 58.26; H, 4.89; N, 10.07. Found: C, 58.22; H, 4.77; N, 10.02%; ESI-MS *m/z*: 557.92 (M^+), 413.12 $[(M^+–CH_2CH_2N{=}CHPhOH)]^+$; ^{1}H NMR (400 MHz, $CDCl_3$, δ, ppm): −25.73, −20.06, −9.17, 7.61, 11.20, 13.89, 17.04 (see Section 3); IR (cm^{-1}, KBr pellet): 3055–2857 (ν_{C-H}), 1600–1531 ($\nu_{C=N}$), 1438, 1242, 1120, 722.

*2.3.2. $[OsL^1]$ (**2**)*

To a hot solution of H_3L^1 (0.046 g, 0.10 mmol) and triethylamine (0.30 g, 0.30 mmol) in warm 2-methoxyethanol (40 mL) was added $[Os(PPh_3)_2Cl_2]$ (0.10 g, 0.10 mmol). The mixture was heated at reflux for 24 h to produce a dark brownish solution. Stripping of the solvent from the solution under vacuum gave a brownish solid, which was subjected to thin-layer chromatography on a silica plate. With acetonitrile:toluene (1:4) as the eluant, a brown band separated out. The brown band was extracted with acetonitrile, and slow evaporation of the acetonitrile extract gave the brown crystalline $[OsL^1]$. Yield: 0.074 g, 50%. *Anal.* Calc. for $C_{27}H_{27}N_4O_3Os$: C, 50.22; H, 4.21; N, 8.68. Found: C, 50.28; H, 4.30; N, 8.79%; ESI-MS *m/z*: 647.75 $(M)^+$; ^{1}H NMR: 7.52–7.56 (broad), 7.10 (broad), 6.73 (broad), 3.16–3.52 (broad), 2.61–2.67 (broad); IR(cm^{-1}, KBr pellet): 3401–2680, 1599, 1456, 1109, 1037, 758.

*2.3.3. $[RuL^2]$ (**3**)*

To a hot solution of H_3L^2 (0.051 g, 0.10 mmol) and triethylamine (0.30 g, 0.30 mmol) in ethanol (40 ml), was added $[Ru(PPh_3)_2Cl_2]$ (0.096 g, 0.10 mmol). The mixture was heated at reflux for 24 h to produce a deep purple solution. Stripping of the solvent from the solution under vacuum gave a greenish solid. Using TLC with acetonitrile:toluene (1:4) as the eluant, a purple band (R_f = 0.6) separated out. The purple band was extracted with acetonitrile, and slow evaporation of the acetonitrile extract gave a purple crystalline solid of the composition $[RuL^2]$. Yield: 0.060 g, 50%. *Anal.* Calc. for $C_{30}H_{39}N_4O_3Ru$: C, 59.58; H, 6.50; N, 9.26. Found: C, 60.03; H, 6.30; N, 9.15%; ESI-MS *m/z*: 607.7 (M^+); ^{1}H NMR (400 MHz, $CDCl_3$, δ, ppm): 3.35–4.5 (complex), 6.0–8.0 (complex), 10.08. IR (cm^{-1}, KBr pellet): 3792–2920, 1614, 1478, 1265, 1093, 755.

*2.3.4. $[OsL^2]$ (**4**)*

To a hot solution of H_3L^2 (50.6 mg, 0.10 mmol) and triethylamine (0.30 g, 0.30-mmol) in 2-methoxyethanol (40 mL), was added $[Os(PPh_3)_2Cl_2]$ (0.10 g, 0.10 mmol). The mixture was heated at reflux for 24 h to produce a light brownish solution. Stripping of the solvent from the solution under vacuum gave a brownish solid, which was subjected to thin-layer chromatography on a silica plate. With acetonitrile as the eluant, a light brown band (R_f = 0.3) separated out. The light brown band was extracted with acetonitrile, and slow evaporation of the acetonitrile extract gave the brown crystalline $[OsL^2]$. Yield: 0.057 g, 42%; *Anal.* Calc. for $C_{30}H_{39}N_4O_3Os$: C, 51.93; H, 5.67; N, 8.07. Found: C, 52.87; H, 5.74; N, 8.12%; ESI-MS *m/z*: 744.59 $(M+K)^+$; ^{1}H NMR (400 MHz, $CDCl_3$, δ, ppm): 2.09, 2.23, 3.2–3.54 (broad), 3.70, 6.7–6.8 (broad), 7.07–7.17 (broad), 7.51–7.68 (complex, broad); IR (cm^{-1}, KBr pellet): 3908–2360, 1637, 1245, 1094, 723.

*2.3.5. $[RuL^3](BPh_4)_2$ (**5**)*

To a hot solution of L^3 (0.041 g, 0.10 mmol) in ethanol (40 mL), $[Ru(PPh_3)_2Cl_2]$ (0.096 g, 0.10 mmol) was added. The mixture was heated to reflux for 24 h, resulting in a dark reddish-brown solution. Evaporation of this solution under vacuum gave a reddish-brown solid, which was dissolved in methanol and $NaBPh_4$ was added. The mixture was again stirred for 30 min. The resulting solution was filtered, and the residue was washed with a little methanol to yield the dark brown colored crystalline complex **5**. Yield: 0.181 g, 65%. *Anal.* Calc. for $C_{72}H_{67}B_2N_7Ru$: C, 75.00; H, 5.86; N, 8.50. Found: C, 74.80; H, 5.94; N, 8.58%; ESI-MS *m/z*: 833.61 (M^+), 514.70 $(M–BPh_4)^+$; ^{1}H NMR (400 MHz, DMSO-d_6, δ, ppm): 10.09 (–CH, 3H), 6.79–8.81 (aromatic ring, complex), 3.49

(t, 6H, NCH_2CH_2), 2.17 (t, 6H, NCH_2CH_2); IR (cm^{-1}, KBr pellet): 3401–2360, 1630, 1587, 1469, 1435, 1151, 736.

*2.3.6. $[Os(L^3)](BPh_4)_2$ (**6**)*

To a hot solution of L^3 (0.041 g, 0.10 mmol) in toluene (40 mL), was added $[Os(PPh_3)_2Cl_2]$ (0.10 g, 0.10 mmol). The mixture was heated to reflux for 24 h, resulting in a dark reddish-brown solution. Evaporation of this solution under vacuum gave a reddish-brown solid, which was dissolved in methanol and $NaBPh_4$ was added. The mixture was again stirred for 30 min. The resulting solution was filtered, and the residue was washed with little methanol to yield the dark maroon colored crystalline complex **6**. Yield: 0.13 g, 43%; *Anal.* Calc. for $C_{72}H_{67}B_2N_7Os$: C, 69.62; H, 5.44; N, 7.89. Found: C, 69.67; H, 5.49; N, 7.93%; ESI-MS *m/z*: 922.56 (M^+). ^1H NMR (400 MHz, DMSO-d_6, δ, ppm): 2.08 (t, 6H, NCH_2CH_2), 3.63 (6H, NCH_2CH_2), 6.74–7.8 (aromatic ring, complex, BPh_4), 8.45 (–CH, 3H). IR (cm^{-1}, KBr pellet): 3368–2359, 1658, 1588, 1477, 1427, 1308, 1152, 845, 734, 706.

*2.3.7. $[Ru(L^4)](BPh_4)_2$ (**7**)*

To a hot solution of L^4 (0.046 g, 0.10 mmol) in ethanol (40 mL), $[Ru(PPh_3)_2Cl_2]$ (0.096 g, 0.10 mmol) was added. The mixture was heated to reflux for 24 h, resulting in a dark reddish-brown solution. Evaporation of this solution under vacuum gave a reddish-brown solid, which was dissolved in methanol and $NaBPh_4$ was added. The mixture was again stirred for 30 min. The resulting solution was filtered, and the residue was washed with little methanol to yield the dark brown colored crystalline complex **7**. Yield: 0.122 g, 47%; *Anal.* Calc. for $C_{75}H_{79}B_2N_7Os$: C, 74.99; H, 6.63; N, 8.16. Found: C, 75.01; H, 6.70; N, 8.24%; ESI-MS *m/z*: 881.72 (M^+); ^1H NMR (400 MHz, DMSO-d_6, δ, ppm): 2.15 (s, 9N–CH_3), 2.50 (complex, 6H), 2.61 (complex, 6H), 3.59 (s, 6CH_2), 6.74–8.50 (complex), 9.05 (3H, –CH). IR (cm^{-1}, KBr pellet): 3436–2360, 1579, 1477, 1092, 734, 706.

*2.3.8. $[Os(L^4)](BPh_4)_2$ (**8**)*

To a hot solution of L^4 (0.046 g, 0.10 mmol) in ethanol (40 mL), $[Os(PPh_3)_2Cl_2]$ (0.10 g, 0.10 mmol) was added. The mixture was heated to reflux for 24 h, resulting in a dark reddish-brown solution. Evaporation of this solution under vacuum gave a reddish-brown solid, which was dissolved in methanol and $NaBPh_4$ was added. The mixture was again stirred for 30 min. The resulting solution was filtered, and the residue was washed with a little methanol to yield the dark maroon colored crystalline complex **8**. Yield: 0.131 g, 47%; *Anal.* Calc. for $C_{75}H_{79}B_2N_7Os$: C, 69.81; H, 6.17; N, 7.60. Found: C, 70.03; H, 6.11; N, 7.49%; ESI-MS *m/z*: 972.75 (M^+); ^1H NMR (400 MHz, DMSO-d_6, δ, ppm): 2.15 (s, 9N–CH_3), 2.50 (complex, 6H), 2.68 (broad, 6H), 3.38 (broad, 6H), 3.63 (s, 6CH_2), 6.76–8.45 (aromatic ring, complex). IR (cm^{-1}, KBr pellet): 3436–2373, 1593, 1469, 1102, 733, 704.

*2.3.9. $[Ru(L^5)](BPh_4)_2$ (**9**)*

To a hot solution of L^5 (0.042 g, 0.10 mmol) in ethanol (40 mL), $[Ru(PPh_3)_2Cl_2]$ (0.096 g, 0.10 mmol) was added. The mixture was heated to reflux for 24 h, resulting in a dark reddish-brown solution. Evaporation of this solution under vacuum gave a reddish-brown solid, which was dissolved in methanol and $NaBPh_4$ was added. The mixture was again stirred for 30 min. The resulting solution was filtered, and the residue was washed with a little methanol to yield the dark brown colored crystalline complex **9**. Yield: 0.145 g, 53%; *Anal.* Calc. for $C_{69}H_{70}B_2N_{10}Ru$: C, 71.32; H, 6.07; N, 12.05. Found: C, 71.34; H, 6.11; N, 12.12%; ESI-MS *m/z*: 842.56 (M^+); ^1H NMR (400 MHz, DMSO-d_6, δ, ppm): 2.32 (6H, NCH_2CH_2), 2.67 (6H, NCH_2CH_2), 3.99 (s, 9H, N–CH_3), 6.75–7.2 (complex, imidazole ring, BPh_4), 8.85 (s, 3H, CH); IR (cm^{-1}, KBr pellet): 3436–2356, 1634, 1579, 1480, 1288, 1128, 844, 734, 706.

*2.3.10. $[Os(L^5)](BPh_4)_2$ (**10**)*

To a hot solution of L^5 (0.042 g, 0.10 mmol) in ethanol (40 mL), $[Os(PPh_3)_2Cl_2]$ (0.10 g, 0.10 mmol) was added. The mixture was heated to reflux for 24 h, resulting in a dark reddish-brown solution. Evaporation of this solution under vacuum gave a reddish-brown solid, which was dissolved in methanol and $NaBPh_4$ was added. The mixture was again stirred for 30 min. The resulting solution is filtered, and the residue was washed with little methanol to yield a dark maroon color crystalline complex **10**. Yield: 0.166 g, 56%; *Anal.* Calc. for $C_{69}H_{70}B_2N_{10}Os$: C, 66.23; H, 5.64; N, 11.19. Found: C, 66.27; H, 5.69; N, 11.34%; ESI-MS *m/z*: 932.61 (M^+); ^1H NMR(400 MHz, DMSO-d_6, δ, ppm): 2.33 (6H, NCH_2CH_2), 2.66 (br, 6H, NCH_2CH_2), 3.92 (s, 9H, N-CH_3), 6.75–7.20 (imidazole ring, BPh_4), 8.90(s, 3H, CH); IR(cm^{-1}, KBr pellet): 3435–2358, 1478, 1427, 1267, 1103, 847, 733, 708.

*2.3.11. $[Ru(L^6)](BPh_4)_2$(**11**)*

To a hot solution of L^6 (0.047 g, 0.10 mmol) in ethanol (40 mL) $[Ru(PPh_3)_2Cl_2]$ (0.096 g, 0.10 mmol) was added. The mixture was heated to reflux for 24 h resulting dark reddish-brown solution. Evaporation of this solution under vacuum gave a reddish-brown solid, which was dissolved in methanol and $NaBPh_4$ was added. The mixture was again stirred for 30 min. The resulting solution was filtered, and the residue was washed with a little methanol to yield the dark brown colored crystalline complex **11**. Yield: 0.157 g, 62%; *Anal.* Calc. for $C_{72}H_{82}B_2N_{10}Ru$: C, 71.46; H, 6.83; N, 11.57. Found: C, 71.29; H, 6.63; N, 11.79%; ESI-MS *m/z*: 890.8 (M^+); ^1H NMR (400 MHz, DMSO-d_6, δ, ppm): 2.87, 2.96, 3.45–3.54 (complex), 6.75–7.45 (complex, BPh_4); IR (cm^{-1}, KBr pellet): 3436–2360, 1579, 1479, 1427, 1279, 1089, 734, 706.

*2.3.12. $[Os(L^6)](BPh_4)_2$ (**12**)*

To a hot solution of L^6 (0.047 g, 0.10 mmol) in ethanol (40 mL), $[Os(PPh_3)_2Cl_2]$ (0.10 g, 0.10 mmol) was added. The mixture was heated to reflux for 24 h, resulting in a dark reddish-brown solution. Evaporation of this solution under vacuum gave a reddish-brown solid, which was dissolved in methanol and $NaBPh_4$ was added. The mixture was again stirred for 30 min. The resulting solution was filtered, and the residue was washed with a little methanol to yield the maroon colored crystalline complex **12**. Yield: 0.117 g, 43%; *Anal.* Calc. for $C_{72}H_{82}B_2N_{10}Os$ Calc: C, 66.55; H, 6.36; N, 10.78. Found: C, 66.58; H, 6.31; N, 10.68%; ESI-MS *m/z*: 1008.53 $(M+K)^+$; ^1H NMR (400 MHz, DMSO-d_6, δ, ppm): 2.10 (s, 9N–CH_3), 2.50 (complex, 6H), 3.53 (s, 9CH_3), 3.69 (s, 9CH_3), 3.80 (s, 3CH_2), 6.7–7.6 (complex, BPh_4); IR (cm^{-1}, KBr pellet): 3434–2362, 1648, 1479, 1285, 1090, 734, 706.

2.4. Physical measurements

IR spectra were obtained on a Perkin–Elmer Spectrum RXI spectrophotometer with samples prepared as KBr pellets. Elemental analyses were performed on a Perkin–Elmer 2400 series II CHN series. Electronic spectra were recorded on a U-4100, HITACHI spectrometer. ^1H NMR spectra were obtained on a Brucker Avance III-500 NMR spectrometer using TMS as the internal standard. Electrochemical measurements were made using a PAR model 273 potentiostat. A platinum disk working electrode, a platinum wire auxiliary electrode and an aqueous saturated calomel reference electrode (SCE) were used in a three electrode configuration. Electrochemical measurements were made under a dinitrogen atmosphere. All electrochemical data were collected at 298 K and are uncorrected for junction potentials. Fluorescence spectra were taken on a HORIBA JOBINYVON spectrofluorimeter. Mass spectra were recorded on a Q-Tof Micromass spectrometer by positive-ion mode electrospray ionization. Optimization of the ground-state structures and energy calculations for all the complexes were car-

Table 1
Crystal data for **1** and **2**.

	1	**2**
Empirical formula	$C_{27}H_{27}N_4O_3Ru$	$C_{27}H_{27}N_4O_3Os$
Formula weight	556.6	645.76
Space group	orthorhombic, *pbca*	monoclinic, *P2(1)/c*
a (Å)	13.4886(7)	12.2154(4)
b (Å)	16.5664(8)	14.3003(5)
c (Å)	24.2155(12)	16.1433(5)
V (Å^3)	5411.1(5)	2817.42(16)
Z	4	2
λ (Å)	0.7107	0.7107
Crystal size (mm^3)	0.25 × 0.15 × 0.10	0.09 × 0.05 × 0.04
T (K)	100	100
μ (mm^{-1})	0.622	4.849
$R[F^2 > 2\sigma(F^2)]$	0.0399	0.0307
$wR(F^2)$	0.074	0.0809
Goodness-of-fit (GOF)	1.126	1.173
w	$1/[\sigma^2(F_o^2) + (0.0046P)^2 + 12.7148P]$ where $P = (F_o^2 + 2F_c^2)/3$	$1/[\sigma^2(F_o^2) + (0.0413P)^2 + 12.2131P]$ where $P = (F_o^2 + 2F_c^2)/3$

ried out with the density functional theory (DFT) method using the GAUSSIAN 03 package [48], restricted and unrestricted (for [RuL^1], [OsL^1], [RuL^2] and [OsL^2]) spin had been considered and where B3LYP [49] was chosen as the basis function, the 631g(d,p) basis set was taken for H, C, N and O, and the SDD basis set for ruthenium and osmium. Optimization was carried out until global minima were achieved.

2.5. Crystallography of *1* and *2*

Single crystals of **1** and **2** were obtained by slow diffusion of dichloromethane into hexane solutions of the complexes. Selected crystal data and data collection parameters are given in Table 1. Crystal Data were collected on a Bruker SMART APEXII CCD area-detector diffractometer using graphite monochromated MoKα radiation (λ = 0.71073 Å). For both the crystals, X-ray data reduction was carried out using the Bruker SAINT program. The structures were solved by direct methods using the SHELXL-97 program [50].

The unit cell dimensions were determined by a least squares fit of 7901 machine centered reflections ($2 < \theta < 25°$) for **1** and 9981 machine centered reflections ($0 < \theta < 38°$) for **2**. Thirty-six standard reflections were used to check the crystal stability towards X-ray exposure, and these showed no significant intensity reduction over the course of the data collection. X-ray data reduction, structure solution and refinement were done using the SHELXL-97 program package. Four final cycles of refinement converged with discrepancy indices $R[F^2 > 2\sigma(F^2)] = 0.0428$ and $wR(F^2) = 0.1311$ for [RuL^1] and $R[F^2 > 2\sigma(F^2)] = 0.0663$ and $wR(F^2) = 0.2246$ for [OsL^1].

3. Results and discussion

All the complexes have been prepared by the direct reaction of tris(2-aminoethyl)amine based heptadentate ligands ($H_3L^{1,2}$, L^3–L^6), and ruthenium or osmium precursors at refluxing temperature. The ruthenium and osmium precursors $[Ru(PPh_3)_3Cl_2]$, $[Ru(CO)_2(PPh_3)_2Cl_2]$, $RuCl_3{\cdot}H_2O$, $(NH_4)_2[OsCl_6]$ and $[Os(PPh_3)_3Cl_2]$ were chosen for the present study. Interestingly, the final products are of the same stoichiometry [ML] (M = Ru, Os; L = H_3L^1, H_3L^2) or $[ML]^{2+}$ (M = Ru, Os; L = L^3–L^6) in every case. The oxidation state of ruthenium and osmium is +3 in [ML] (L = H_3L^1, H_3L^2) and +2 in $[ML]^{2+}$ (L = L^3–L^6), irrespective of the ruthenium or osmium precursors chosen, and the ligands were able to displace phosphine, carbonyl and halogens efficiently. The $[ML]^{2+}$ (L = L^3–L^6) complexes have been precipitated from solution as the tetraphenylborate salt. The ligands and the complexes were characterized by the usual techniques: elemental analyses, infrared spectra, ^{1}H NMR and ESI-MS. Moreover, The X-ray structures for two of the complexes were determined. The potentially heptadentate ligands $H_3L^{1,2}$ are coordinated as a trianionic hexadentate ligand, whereas L^3–L^6 are coordinated as a neutral hexadentate ligand (Fig. 2). The tertiary amine nitrogen atom remains uncoordinated in all the complexes. The complexes **1**–**12** are stable in air. They are soluble in a wide variety of solvents, like methanol, dichloromethane, chloroform DMF, DMSO, acetonitrile and acetone.

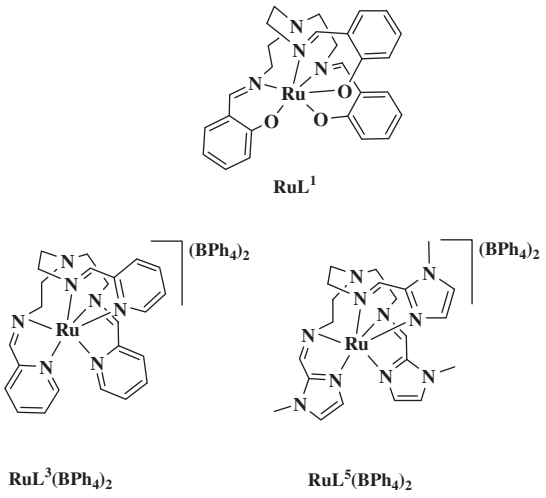

Fig. 2. Predicted coordination environment around the metal.

3.1. Description of the crystal structure

Single crystals of complexes **1** and **2**, suitable for X-ray diffraction studies, were grown by crystallization from dichloromethane–hexane solution. The molecular structures and atom numbering schemes of **1** and **2** are presented in Fig. 3. The crystallographic data and structure analysis for complexes **1** and **2** are summarized in Table 1 and selected bond distances and bond angles are given in Table 2. The X-ray results show that the heptadentate H_3L^1 is coordinated via three imino nitrogen [N2, N3, N4] and three oxygen atoms [O1, O2, O3, formed through deprotonation of the OH groups] to the metal, which resides in a distorted octahedral environment. The nitrogen atom N1 (sp^3 hybridized), which sits on the top, does not have any bonding interaction with ruthenium or osmium. The crystal structure of **1** has been solved previously, but

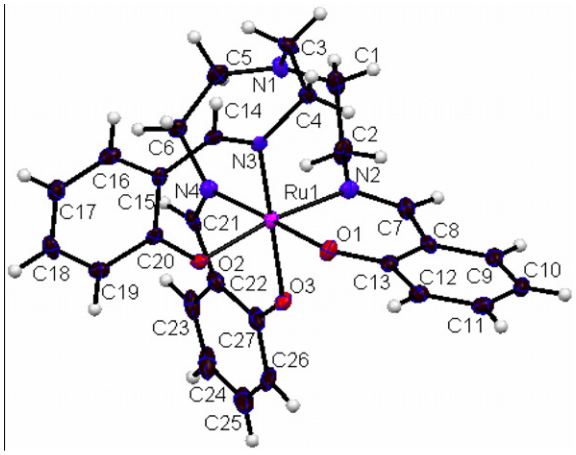

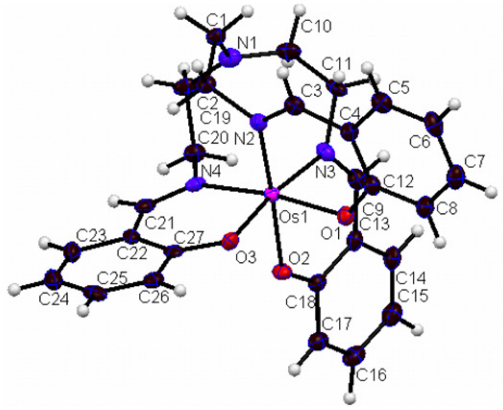

Fig. 3. Molecular view of **1** and **2**.

Table 2
Selected bond lengths (Å) and bond angles (°) of **1** and **2**.

Bond lengths	Bond angles	Bond angles
1		
Ru1–O2 1.999(2)	O2–Ru1–O3 85.03(9)	O1–Ru1–N3 84.87(10)
Ru1–O3 2.018(2)	O2–Ru1–O1 87.88(10)	N4–Ru1–N3 93.70(11)
Ru1–O1 2.027(2)	O3–Ru1–O1 88.22(10)	O2–Ru1–N2 171.17(10)
Ru1–N4 2.039(3)	O2–Ru1–N4 89.03(10)	O3–Ru1–N2 86.28(11)
Ru1–N3 2.058(3)	O3–Ru1–N4 92.93(11)	O1–Ru1–N2 90.29(11)
Ru1–N2 2.070(3)	O1–Ru1–N4 176.60(11)	N4–Ru1–N2 92.97(11)
	O2–Ru1–N3 89.86(10)	N3–Ru1–N2 98.59(11)
	O3–Ru1–N3 171.55(11)	
2		
Os1–O1 2.022(4)	O1–Os1–O3 84.95(14)	O2–Os1–N3 91.59(15)
Os1–O3 2.028(3)	O1–Os1–O2 86.03(13)	N2–Os1–N3 94.96(16)
Os1–O2 2.035(3)	O3–Os1–O2 86.34(14)	O1–Os1–N4 172.26(15)
Os1–N2 2.043(4)	O1–Os1–N2 92.06(15)	O3–Os1–N4 91.33(16)
Os1–N3 2.049(4)	O3–Os1-N2 86.86(15)	O2–Os1–N4 86.96(14)
Os1–N4 2.054(4)	O2–Os1–N2 173.07(14)	N2–Os1–N4 94.51(15)
	O1–Os1–N3 86.65(16)	N3–Os1–N4 96.83(17)
	O3–Os1–N3 171.47(15)	

with different a solvent [41]. A literature survey shows that the average Ru–N(O) bond length relevant to salen corresponds to 2.01 Å, and this is a little higher (2.034 Å) in our case [51,52]. The angles around the ruthenium center deviate significantly from 90°. The N2–Ru1–N3, N3–Ru1–N4, O3–Ru1–N4 and N2–Ru1–N4 angles have opened up to 98.59(11)°, 93.70(11)°, 92.93(11)° and 92.97(11)° and the O2–Ru1–O3, O1–Ru1–N3, O3–Ru1–N2 and O1–Ru1–O2 angles have reduced to 85.03(10)°, 84.87(10)°, 86.28(11)° and 87.88(10)°, indicating distortion from a regular octahedron. For the [Os(III)L^1] complex, the deviation is significant. Here, the N3–Os1–N4, N2–Os1–N4, N2–Os1–N3 angles have opened up to 96.83(16)°, 94.51(14)°, and 94.96(16)° and all other angles around Os1 have significantly reduced, of which the O1–Os1–O3 angle of 84.95(13)° is the smallest. The Os–O and Os–N bond lengths are quite normal and comparable with similar type osmium(III) complexes [53,54]. Both the structures have disorders in the solvent molecule.

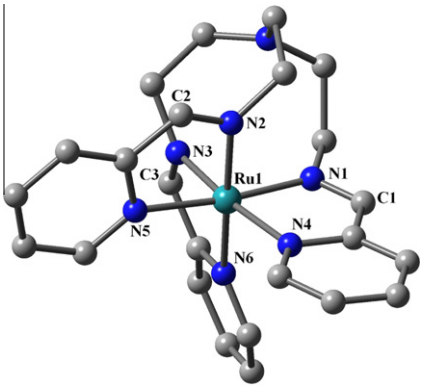

Fig. 4. Geometry optimized structure of complex **5**.

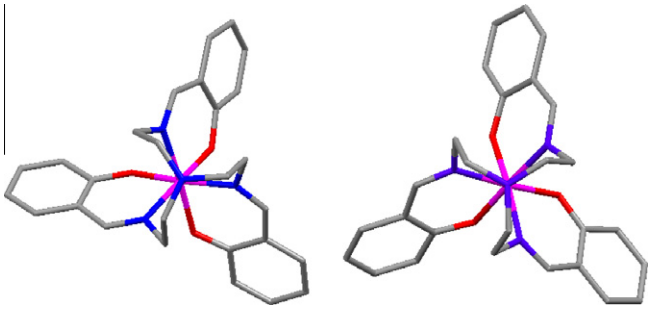

Fig. 5. Δ-(clockwise) and Λ-(anticlockwise) enantiomorphs due to the screw arrangement of the tripod type ligand around the Ru(II) and Os(II) ions.

To get an idea about the trapped ruthenium and osmium centers in the tripodal ligands H_3L^2 and L^3–L^6, geometry optimization calculations were carried out using GAUSSIAN 03. The metal ion is definitely surrounded by three Schiff base (imine) nitrogen and three pyridine/imidazole nitrogen atoms in an octahedral fashion, and the tertiary amine nitrogen atom is uncoordinated. A literature survey shows there is not a single report on ruthenium or osmium complexes with the ligands L^3–L^6. However, the crystal structure of [FeL^3]$(ClO_4)_2$ has been reported by Brewer et al. [54], and our calculated bond parameters are in very good agreement with the reported figures, with a bit lengthier Os–N bond. The geometry optimized structure of complex **5** is given in Fig. 4. The obtained bond parameters around the metal center are found to be quiet comparable with the structure reported by Yamaguchi et al. [40] for complexes **9**–**12**. The change of the sp^2 nitrogen(imine) in **9** to the sp^3 nitrogen(reduced imine) in **11** is reflected by the change in the average Ru–N(imine) bond length of 2.274 to 2.291 Å. Bond parameters (Tables S1–S3) and optimized figures (Figs. S1–S9) are deposited in Supporting information.

3.2. Electrospray ionization mass spectrometry (ESI-MS)

Elemental analysis and ESI-MS confirmed the formation of the ligands ($H_3L^{1,2}$, L^3–L^6) and of complexes **1**–**12** with definite stoichi-

Table 3
Electrochemical and spectral data of the ligands and complexes.

Complex	Electronic spectral data λ_{max} (nm) ($\epsilon \times 10^{-4}$, L mol^{-1} cm^{-1})[a]	Cyclic voltammetric data,[b] *E*, *V* vs. SCE	Fluorescence[a]	
			Excited at (nm)	Emission at (nm)
1	626(1.26), 402(6.36), 327(11.66), 264(53)		264	363 (vibrational fine structure)
			396	427, 453
2	410(5.67), 330(10.01)	1.0844[d],	258	298
		−0.6743[e], −1.0225[e]	406	no peak
3	326(5.09), 358(3.32), 546(2.40)	−0.886($E_{1/2}$)[c]	270	303, 398
			546	no peak
4	846(.022), 345(0.18), 272(0.70)	1.029[d], −1.1152[e]	264	308
				416 (weak)
5	464(2.45), 380(3.16), 264(13.49)	1.1441[d]	260	301, 431
6	476(5.47), 440(4.53), 336(5.83)	1.1018[d], −0.6516[e]	476	534 (broad peak)
7	362(11.03)	0.8629, −1.1867 ($E_{1/2}$)[c]	260	430
8	478(2.68), 338(2.85)	1.045[d]	220	337, 396
			270	515
9	442(4.40), 292(4.79)	1.1032[d], −0.7589[e]	292	344
			450	no peak
10	270(8.67), 428(0.69)	1.1097[d]	270	307
			410	485
11	382(2.92)	0.9736[d]	380	no peak
			224	338
12	417(0.42), 358(0.96), 321(1.30)	0.835[d], −0.682[e]	224	337, 401

[a] Electronic spectral data of the ligands in acetonitrile.
[b] Supporting electrolyte, TBAP; reference electrode, SCE; scan rate, 50 mV s^{-1}.
[c] $E_{1/2} = 0.5(E_{pa} + E_{pc})$, where E_{pa} and E_{pc} are the anodic and cathodic peak potentials.
[d] E_{pa}.
[e] E_{pc}.

ometry. The presence of a peak (*m/z*) at 458.88, 414.83 and 422.89 for H_3L^1, L^3 and L^5 confirm the formation of the ligand through condensation of tris(2-aminoethyl)amine and the corresponding aldehyde in a 1:3 M ratio. Simple reduction by $NaBH_4$ and subsequent N-methylation give rise to the ligands H_3L^2, L^4 and L^6, marked by the peaks (*m/z*) at 506.77, 461.97 and 470.96. The analysis of the higher mass region of the spectra for the complexes formed by the synthesized ligands show a signal attributable to the presence of [ML] (M = Ru, Os; L = H_3L^1, H_3L^2) or $[ML]^{2+}$ (M = Ru, Os; L = L^3–L^6) in the sample. The metal/organic ligand ratio observed is 1:1 for all the complexes. The molecular ion peaks are present for all the complexes at the respective *m/z* values, with the expected isotope distribution patterns calculated for the ruthenium and osmium complexes respectively. Generally, $[ML]^{2+}$ type complexes show a molecular ion peak at $ML(BPh_4)^+$. In addition, some $[ML(BPh_4)_2]$ complexes also show peaks corresponding to the composition $[ML]^+$ or at [ML+cation] [cation = Na^+ or K^+]. Two representative mass spectra for **7** and **12** are shown in Fig. S10.

3.3. CD spectra

The CD spectra of **1**–**3** clearly indicate the presence of a racemic mixture for each complex in solution. As resolution does not occur spontaneously during the course of crystallization, an optically active auxiliary agent for resolution is required. Each complex contains mixture of Δ (clockwise) and Λ (anticlockwise) enantiomorphs, depending on the screw arrangement of the tripod-type ligand around the metal ion. Optical resolution for the complexes is in progress. However, the particular crystal of **1** is a Δ-enantiomorphs, and for complex **2**, it is an Λ-isomer. The screw arrangements of the ligands around the metal have been shown in Fig. 5.

3.4. NMR spectra

The ^{1}H NMR spectra clearly establish the diamagnetism of all the complexes, except [ML] (M = Ru, Os; L = H_3L^1, H_3L^2) (see Section 2). The spectra exhibited by the [ML] (M = Ru, Os) (L = H_3L^1, H_3L^2)} complexes are not well resolved, and are broad and ill defined as expected for Ru(III) and Os(III) complexes. The spectrum of **1** is shown in Fig. S3 (Supporting information). For the complexes $[ML](BPh_4)_2$ (M = Ru, Os; L = L^3–L^6), having tetraphenyl borate anion, the assignment of signals could not be made with confidence due to the overlapping of peaks in the aromatic region.

3.5. Infrared spectra

The infrared (IR) spectra for the series of ligands and compounds were measured at ambient temperature as KBr pellets. The IR spectra of the ligand H_3L^1 and H_3L^2 are characterized by an intense band attributable to the O–H stretching at 3436 cm^{-1} (broad) [55], typical for intramolecular hydrogen bonded O–H. This broad feature is absent in the complexes **1**–**4**. For, $H_3L^{1,2}$ and L^3–L^6 characteristic bands attributable to C–H stretching at 3400–2352 cm^{-1} and for H_3L^1, $L^3$and L^5 bands at1632–1651 cm^{-1} ($\nu_{C=N}$) are present. These bands are absent in the corresponding N-methylated ligands.

3.6. Electronic spectra

The absorption and emission spectra of all the ligands and complexes were performed in acetonitrile solution (Table 3). The ligands absorb mainly in the ultra-violet region. The complexes show bands in the visible region as well as in the ultraviolet region. The characteristics emission spectra of the ligands and complexes are shown in Fig. S4 (Fig. 6 [56]).[1] All the complexes have essentially started with the tris-(2aminoethyl)amine moiety, which emits in the region between 525 and 625 nm. The ligands L^1 and L^3 show strong a emission which is blue shifted to the 400–500 nm region, while the emission intensity is quite high in the case of L^3. It can be seen that the reduction of –C=N and subsequent N-methylation changes the emission pattern completely.

[1] Fig. 6 represents the emission spectra of the ligand L^3, complex **5** and complex **6**.

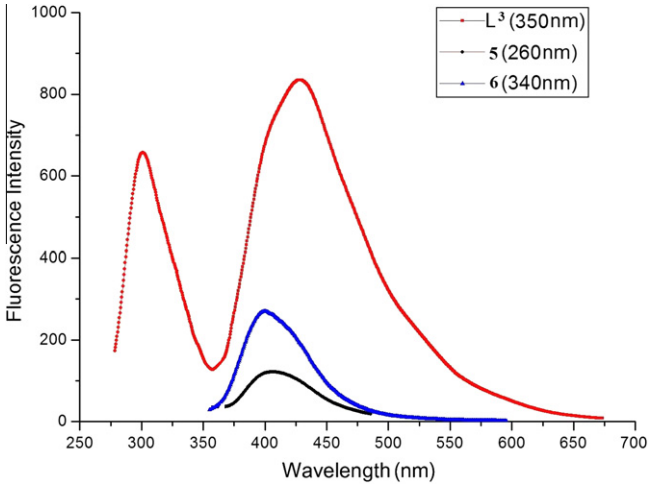

Fig. 6. Emission pattern of ligand L^3 and complexes **5** and **6**.

So, it is obvious that the change in the π–π^* transition is attributed to the change in the fluorescence pattern [57]. The ruthenium complexes fluoresce more strongly than the corresponding osmium complexes, except for complex **9** in our case. For the complexes, emissions arising from metal centered excited states of MLCT character are expected since ruthenium and osmium are easy to oxidize or reduce [58]. Quenching of fluorescence by transition metal ions during complexation is a common phenomenon which is explained by processes such as magnetic perturbation, redox activity, electronic energy transfer, etc. [59,60]. The complex [OsL^6] shows a complete quenching of fluorescence. For complexes **5** and **7** a new peak arises in the blue-shifted region. This may be attributed to the presence of an additional chromophoric group, >C═N, of the pyridine [61].

To get the idea about the intense lowest-energy absorption for all the twelve complexes, DFT calculations have been performed. From the results, it was found that in [RuL^1] and its osmium analogue, the highest occupied molecular orbital (HOMO) is mostly distributed over the metal center and the lowest unoccupied molecular orbital (LUMO) has predominant ligand character. Hence the lowest-energy absorption is assignable to a metal-to-ligand charge transfer (MLCT) transition, taking place from the filled d-orbital of the metal to the vacant π^*-orbital of the imine ligand. For the ruthenium and osmium complexes of ligands L^2 and L^3, both the HOMO and LUMO contain major contributions from the ligand, but still the metal has a significant contribution as well as the ligand. So the transition may be attributed to an intra ligand transition. For the complexes of ligands $L^{4–6}$, both the HOMO and LUMO have predominant ligand character. Hence the lowest energy transition is assignable to a ligand to ligand charge transfer (LLCT) transition. Polypyridyl complexes of Ru and Os are excellent fluorophores owing to their strong absorption in the visible region and emission at low energy, originating from the spin-forbidden metal-to-ligand charge transfer (MLCT) transitions [62,63]. It is likely that the emission originates from the lowest energy metal to ligand charge transfer (MLCT) state, probably derived from the excitation involving a $d\pi(Ru) \rightarrow \pi^*$(imine) MLCT transition [64]. The electron distribution in the highest occupied molecular orbital (HOMO) and the lowest unoccupied molecular orbital (LUMO) for complex **2** is shown in Fig. 7. The composition of these molecular orbitals for all the complexes is given in Table 4. It is interesting to note that the osmium complexes have a comparatively better metal contribution in the HOMO. Probably the existence of more metal character is responsible for the lower fluorescence of the osmium species.

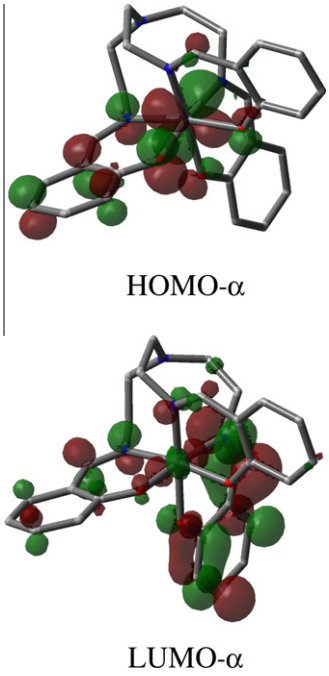

Fig. 7. Partial molecular orbital diagram of complex **2**.

Table 4
Composition of selected molecular orbitals of the ruthenium and osmium complexes.

Complex	Contributing fragments	% Contribution of fragments to	
		HOMO	LUMO
1	Ru	62.67	20.22
	L^1	37.33	79.78
2	Os	68.05	23.24
	L^1	31.95	76.76
3	Ru	23.98	6.07
	L^2	76.02	93.93
4	Os	32.59	9.64
	L^2	67.41	90.36
5	Ru	38.82	8.35
	L^3	61.78	91.65
6	Os	43.59	11.46
	L^3	56.41	88.54
7	Ru	18.03	11.58
	L^4	81.97	88.42
8	Os	23.03	14.61
	L^4	76.97	85.39
9	Ru	17.75	10.98
	L	82.25	89.02
10	Os	20.67	13.54
	L^5	79.33	86.46
11	Ru	19.67	8.71
	L^6	80.33	91.29
12	Os	24.98	12.37
	L^6	75.02	87.63

3.7. Cyclic voltammetry

Cyclic voltammograms (CV) of all the complexes were recorded in dichloromethane–acetonitrile (1:9) (0.1 M TBAP), and the data are summarized in Table 3. The cyclic voltammograms of **1**–**4** are quite similar. All of these complexes exhibit one metal-based irreversible oxidation in the range 0.95–1.08 V. In view of the composition of the HOMO in these complexes, the first oxidative response is assigned to Ru(III)/Ru(IV) oxidation. Complexes **5**–**12** show a common irreversible oxidation peak in the range 0.86–1.14 V. Again, based on the composition of HOMO, these peaks are attrib-

utable to oxidation of Ru(II/III), whereas the peak at 1.94 V for complex **6** is purely ligand based.

4. Conclusion

In summary, we have shown that the reaction of tris(2-aminoethyl)amine based ligands with ruthenium and osmium precursors result in the formation of mononuclear complexes of the general formula [ML] or $[ML]^{2+}$, which have been characterized by different spectroscopic techniques and cyclic voltammetry. The X-ray structures of **1** and **2** have been reported. This is the first crystallographically characterized osmium complex of tris(2-aminoethyl)amine based ligands. The ligands, as well as the complexes, have very good emissive properties. The electronic spectra, TD-DFT method and the transitions' characters were discussed in connection with the structure of the molecular orbitals of the complexes. Optical resolutions for the complexes are in progress.

Acknowledgements

PG would like to thank the Department of Science and Technology, India, research Grant SR/FT/CS-057/2009. S.M. and D.K.S. (9/096(0511)/2006-EMR-I) thank the Council of Scientific and Industrial Research, New Delhi, India for their PhD fellowships. The authors would like to thank Dr. Tapan Kanti Paine and Prof. Soumen Basak and for their help and Mr. G. Ramakrishna for the data collection.

Appendix A. Supplementary data

CCDC 795997 and 795084 contain the supplementary crystallographic data for compound **1** and **2**. These data can be obtained free of charge via http://www.ccdc.cam.ac.uk/conts/retrieving.html, or from the Cambridge Crystallographic Data Centre, 12 Union Road, Cambridge CB2 1EZ, UK; fax: (+44) 1223 336 033; or e-mail: deposit@ccdc.cam.ac.uk. Supplementary data associated with this article can be found, in the online version, at doi:10.1016/j.poly.2011.09.010.

References

[1] D.F. Cook, D. Cummins, E.D. McKenzie, J. Chem. Soc., Dalton Trans. (1976) 1369.
[2] D. Moon, M. Soo Lah, R.E. Del Sesto, J.S. Miller, Inorg. Chem. 41 (2002) 4708.
[3] A.G. Blackman, Polyhedron 24 (2005) 1.
[4] A.K. Phukan, A.K. Guha, Inorg. Chem. 50 (2011) 1361.
[5] A.P. Bouteillb, L. Lamandk, L. Lopez, L. Cazaux, J. Bellan, Tetrahedron 54 (1998) 3817.
[6] S. Panda, P.B. Pati, S.S. Zade, Chem. Comm. 47 (2011) 4174.
[7] H.S. Chong, H.A. Song, X. Ma, S. Lim, X. Sun, S.B. Mhaske, Chem. Commun. (2009) 3011.
[8] D.R. Reddy, Bioconjug. Chem. 22 (2011) 1402.
[9] P.L. Jones, A.J. Amoroso, J.C. Jeffery, J.A. McCleverty, E. Psillakis, L.H. Rees, M.D. Ward, Inorg. Chem. 36 (1997) 10.
[10] C. Paul-Roth, K. Raymond, Inorg. Chem. 34 (1995) 1408.
[11] W. Zhang, Z.Q. Wang, O. Sato, R. Xiong, Cryst. Growth Des. 9 (2009) 2050.
[12] M. Zehnder, U. Thewalt, S. Fallab, Helv. Chim. Acta 62 (1979) 2099.
[13] K.S. Hagen, W.H. Armstrong, H. Hope, Inorg. Chem. 27 (1988) 967.
[14] S.S. Massoud, H. Chun, I. Bernal, J. Coord. Chem. 55 (2002) 619.
[15] I.P.Y. Shek, T.-C. Lau, W.-T. Wong, J.-L. Zuo, New J. Chem. 23 (1999) 1049.
[16] V. Marvaud, C. Decroix, A. Scuiller, C. Guyard-Duhayon, J. Vaissermann, F. Gonnet, M. Verdaguer, Chem. Eur. J. 9 (2003) 1677.
[17] R.M. Hartshorn, D.A. House, J. Chem. Soc., Dalton Trans. 1 (1998) 2577.
[18] J. Jazwinski, J.-M. Lehn, D. Lilienbaum, R. Ziessel, J. Guilhem, C. Pascard, J. Chem. Soc., Chem. Commun. 1 (1987) 1691.
[19] S.J. Archibald, A.J. Blake, S. Parsons, M. Schroder, R.E.P. Winpenny, J. Chem. Soc., Dalton Trans. 1 (1997) 173.
[20] I. Katsuki, Y. Motoda, Y. Sunatsuki, N. Matsumoto, T. Nakashima, M. Kojima, J. Am. Chem. Soc. 124 (2002) 629.
[21] S.P. Yang, H.M. Chen, F. Zhang, X. Bin Yu, Appl. Organomet. Chem. 18 (2004) 88.
[22] E. Ristenpart, Berichte 29 (1896) 2526.
[23] J. Hukkamäki, T.T. Pakkanen, Micropor. Mesopor. Mater. 65 (2003) 189.
[24] A. Grafe, K. Haupt, G.J. Mohra, Anal. Chim. Acta 565 (2006) 42.
[25] P. Krajnc, J.F. Brown, N.R. Cameron, Org. Lett. 4 (2002) 2497.
[26] Z. Zhang, F. Rong, Y. Xie, Y. Wang, H. Yang, D. Fu, J. Nanosci. Nanotechnol. 11 (2011) 2163.
[27] Y. Sumi, M.T. Itoh, T. Muraki, T. Suzuki, Histochem. Cell Biol. 106 (1996) 223.
[28] C. Ma, N. Nakamura, M. Hattori, Chem. Pharm. Bull. 49 (2001) 915.
[29] S.R. Collinson, D.E. Fenton, Coord. Chem. Rev. 148 (1996) 19.
[30] M. Figuet, M.T. Averbuch-Pouchot, A. du M. d'Hardemare, O. Jarjayes, Eur. J. Inorg. Chem. 1 (2001) 2089.
[31] N.W. Alcock, D.F. Cook, E.D. McKenzie, J.M. Worthington, Inorg. Chim. Acta 38 (1980) 107.
[32] W.K. Wong, H. Liang, J. Guo, W.Y. Wong, W.K. Lo, K.F. Li, K.W. Cheah, Z. Zhou, W.T. Wong, Eur. J. Inorg. Chem. 2004 (2004) 829.
[33] P. Dröse, J. Gottfriedsen, Z. Anorg. Allg. Chem. 634 (2008) 87.
[34] M. Allevi, M. Bonizzoni, L. Fabbrizzi, Chem. Eur. J. 13 (2007) 3787.
[35] M.H. Lim, S.J. Lippard, Acc. Chem. Res. 40 (2007) 41.
[36] P.D. Beer, Acc. Chem. Res. 31 (1998) 71.
[37] M.K.D. Armond, M.L. Myrick, Acc. Chem. Res. 22 (1989) 364.
[38] L. Fabbrizzi, A. Leone, A. Taglietti, Angew. Chem. Int. Ed. 40 (2001) 3066.
[39] G.D. Santis, L. Fabbrizzi, M. Licchelli, A. Poggi, A. Taglietti, Angew. Chem. Int. Ed. 35 (1996) 202.
[40] T. Yamaguchi, K. Harada, Y. Sunatsuki, M. Kojima, K. Nakajima, N. Matsumoto, Eur. J. Inorg. Chem. (2006) 3236.
[41] S. Deoghoria, S. Sain, T.K. Karmakar, S.K. Bera, S.K. Chandra, J. Ind. Chem. Soc. 79 (2002) 857.
[42] K. Yamashita, M. Kawano, M. Fujita, K. Yamashita, M. Kawano, M. Fujita, Chem. Commun. (2007) 4102.
[43] F. Schramm, V. Meded, H. Fliegl, K. Fink, O. Fuhr, Z. Qu, W. Klopper, S. Finn, T.E. Keyes, M. Ruben, Inorg. Chem. 48 (2009) 5677.
[44] T.A. Stephenson, G. Wilkinson, J. Inorg. Nucl. Chem. 28 (1966) 945.
[45] P.R. Hoffman, K.G. Caulton, J. Am. Chem. Soc. 97 (1975) 4221.
[46] P. Halder, E. Zangrando, T.K. Paine, J. Chem. Soc., Dalton Trans. 1 (2009) 5386.
[47] M.J. Frisch, G.W. Tracks, H.B. Schlegel, G.E. Scuseria, M.A. Robb, J.R. Cheeseman Jr., J.A. Montgomery, T. Vreven, K.N. Kudin, J.C. Burant, J.M. Millam, S.S. Iyengar, J. Tomasi, V. Barone, B. Mennucci, M. Cossi, G. Scalamani, N. Rega, G.A. Petersson, H. Nakatsuji, M. Hada, M. Ehara, K. Toyota, R. Fukuda, I. Hasegawa, M. Ishida, T. Nakajima, Y. Honda, O. Kitao, H. Nakai, M. Klene, X. Li, J.E. Knox, H.P. Hratchian, J.B. Cross, V. Bakken, C. Adamo, J. Jaramillo, R. Gomperts, R.E. Stratmann, O. Yazyev, A.J. Austin, R. Cammi, C. Pomelli, J.W. Ochterski, P.Y. Ayala, K. Morokuma, G.A. Voth, P. Salvador, J.J. Dannenberg, V.G. Zakrzewski, S. Dapprich, A.D. Daniels, M.C. Strain, O. Farkas, D.K. Malick, A.D. Rabuck, K. Raghavachari, J.B. Foresman, J.V. Ortiz, Q. Cui, A.G. Baboul, S. Clifford, J. Cioslowski, B.B. Stefanov, G. Liu, A. Liashenko, P. Piskroz, I. Komaromi, R.L. Martin, D.J. Fox, T. Keith, M.A. Al-Laham, C.Y. Peng, A. Nanayakkara, M. Challacombe, P.M.W. Gill, B. Johnson, W. Chen, M.W. Wong, C. Gonzalez, J.A. Pople, GAUSSIAN 03, revision D01, Gaussian Inc., Pittsburgh, PA, 2003.
[48] A.D. Becke, J. Chem. Phys. 98 (1993) 5648.
[49] G.M. Sheldrick, Acta. Cryst. A64 (2008) 112.
[50] A. Ahmed, S.D. Robinson, M.F. Uttley, J. Chem. Soc., Dalton Trans. 1 (1972) 843.
[51] F. Pointillart, K. Bernot, J. Colas, L. Sorace, R. Sessoli, Inorg. Chim. Acta 361 (2008) 3427.
[52] J.H. Yoon, H.S. Yoo, H.C. Kim, S.W. Yoon, B.J. Suh, C.S. Hong, Inorg. Chem. 48 (2009) 816.
[53] C.F. Leung, D.T.Y. Yiu, W.T. Wong, S.M. Peng, T.C. Lau, Inorg. Chim. Acta 362 (2009) 3576.
[54] G. Brewer, C. Luckett, L. May, A.M. Beatty, W.R. Scheidt, Inorg. Chim. Acta 357 (2004) 2390.
[55] R.M. Silverstein, F.X. Webster, D.J. Kiemle, Spectroscopic Identification of Organic Compounds, seventh ed., Wiley, 2005.
[56] K. Asai, G. Konishi, K. Sumi, S. Kawauchi, Polym. Chem. 1 (2010) 321.
[57] B.A. Gregg, A. Heller, J. Phys. Chem. 95 (1991) 5976.
[58] Y. Xiao, V. Pavlov, B. Shlyahovsky, I. Willner, Chem. Eur. J. 11 (2005) 2698.
[59] N. Chattopadhyay, A. Mallick, S. Sengupta, J. Photochem. Photobiol. A177 (2006) 55.
[60] P. Purkayastha, G.K. Patra, D. Datta, N. Chattopadhyay, Ind. J. Chem. A 39 (2000) 375.
[61] Y.V. Korovin, R.N. Lozitskaya, N.V. Rusakova, Russ. J. Gen. Chem. 73 (2003) 1641.
[62] V. Balzani, S. Campagna, G. Denti, A. Juris, S. Serroni, M. Venturi, Acc. Chem. Res. 31 (1998) 26.
[63] H. Dürr, S. Bossmann, Acc. Chem. Res. 34 (2001) 905.
[64] V.W. Yam, B.W. Chu, C. Ko, K. Cheung, J. Chem. Soc., Dalton Trans. (2001) 1911.